arXiv:1403.0152v1 [cond-mat.mtrl-sci] 2 Mar 2014

Capillary instability in nanowire geometries

T. Frolov[1], W. C. Carter[2] and M. Asta[1]

March 4, 2014

[1] Department of Materials Science and Engineering, University of California, Berkeley, California 94720, USA

[2] Department of Materials Science and Engineering, Massachusetts Institute of Technology, Cambridge, MA 02139, USA

The vapor-liquid-solid (VLS) mechanism [1] has been applied extensively as a framework for growing single-crystal semiconductor nanowires for applications spanning optoelectronic, sensor and energy-related technologies [2, 3]. Recent experiments have demonstrated that subtle changes in VLS growth conditions produce a diversity of nanowire morphologies, and result in intricate kinked structures that may yield novel properties [4–8]. These observations have motivated modeling studies that have linked kinking phenomena to processes at the triple line between vapor, liquid and solid phases that cause spontaneous "tilting" of the growth direction. Here we present atomistic simulations and theoretical analyses that reveal a tilting instability that is intrinsic to nanowire geometries, even in the absence of pronounced anisotropies in solid-liquid interface properties. The analysis produces a very simple conclusion: the transition between axisymmetric and tilted triple lines is shown to occur when the triple line geometry satisfies Young's force-balance condition. The intrinsic nature of the instability may have broad implications for the design of experimental strategies for controlled growth of crystalline nanowires with complex geometries.

Recent experimental and modeling studies have expanded the theoretical understanding of the thermodynamic and kinetic factors underlying the process of VLS growth, and the origins of observed changes in growth morphologies. In this context, the modeling studies have investigated the geometry of wetting of liquid droplets on faceted nanowires, and have demonstrated transitions between axisymmetric and non-axisymmetric wetting configurations [9–13]. It has been shown that liquid droplet de-pinning from the corners of a rigid nanowire occurs simultaneously with the onset of a tilted (or, kinked) growth morphology [13]. Experimental studies of kink formation in VLS growth have demonstrated that such tilting is accompanied by changes in the orientation and shape of the solid-liquid interface [6], and such observations have been reproduced in computational models of nanowire growth that assume highly anisotropic solid-liquid interface properties [14–16]. While these continuum models have succeeded in reproducing the key features of kinking and tilting processes in VLS growth, they rely on assumptions about processes at the vapor-liquid-solid triple line that are difficult to verify directly from experimental observations. Furthermore, it is difficult to distill a simple explanation that directly conveys to process design and control.

In this paper, we report the results of three-dimensional molecular-dynamics (MD) simulations for a model system consisting of a diamond cubic solid with {211} side-walls and a [111] nanowire axis wetted by a liquid droplet in a VLS geometry (see Methods section for details). In addition, we produce a model that results in a

simple physical explanation for the onset of tilting.

Figure 1 shows a snapshot from the current MD simulations illustrating an equilibrated nanowire configuration. The simulations reveal a complex geometry associated with the wetting of the crystal surfaces. Figure 1a demonstrates that the contact line (i.e., the solid, liquid and vapor (vacuum) phases' triple line) dips below one facet indicated by $\boxed{2}$ and climbs above the neighboring facet labeled as $\boxed{1}$. These triple lines on facets $\boxed{1}$ and $\boxed{2}$ are formed by interfaces with different crystallographic orientations (c.f., Figure 1b). The anisotropy of interface free energies is known to produce such triple line "rumpling". [17]

The 3d geometry of the solid-liquid interface is illustrated in Figure 1c which features four $\{111\}$ faceted orientations separated by interfaces that appear atomically rough in nature. The figure also shows the presence of three $\{111\}$ solid-vapor surfaces adjacent to the "raised" contact lines. These facets are qualitatively similar to the sawtooth geometries commonly reported for VLS growth of Si nanowires using Au catalysts. [18]

The wetting geometry shown in Figure 1 involves contact angles that vary with the volume of the liquid (V_l), as illustrated in Figure 2. It is evident from the figure that the angle between solid-liquid and vapor-liquid interfaces (ϕ_{vs}) increases with increasing size of the liquid droplet. We compare the nanowire contact angles ϕ_{vs} and ϕ_{lv} with equilibrium wetting angles of an isolated liquid droplet on a $\{111\}$ surface, ϕ_{vs}^{Young} and ϕ_{lv}^{Young}, shown in Figure 2c in blue and magenta, respectively. We find that for the range of liquid volumes where ϕ_{vs} is less than ϕ_{vs}^{Young}, the symmetric configurations are observed to remain stable in the simulations. However, as nanowire contact angles approach the Young's values with increasing liquid volume, we observe a spontaneous tilting of the droplet to the side of the nanowire. We were unable to observe stable equilibrium configurations with $\phi_{vs} > \phi_{vs}^{Young}$. The model presented below yields the same result, but for a simplified geometry.

Figure 3 shows the nature of the tilting process. The initial step involves tilting towards the $[11\bar{2}]$ direction, forming a large $(\bar{1}11)$ solid-liquid interface facet. This observation is in qualitative agreement with experiments [6] and previous mesoscale simulations. However, as time progresses the droplet does not lock into a new equilibrium wetting configuration, but rather continues to advance along the nanowire surface (c.f., top panels of Figure 3), while the center of mass of the droplet rotates towards a different facet (c.f., middle panels). During this process the shape of the solid-liquid interface evolves on the same time scale as shown in the bottom panel of Figure 3. Specifically, during the process the solid part of the nanowire covered by liquid increases and becomes more spherical. The top part of the nanowire remains wetted in this process and the unpinning of the droplet never occurs in the simulation. This behavior is qualitatively distinct from the assumptions underlying recent models that consider wetting transitions on fixed solid shapes [13].

To further explore the correlation between the tilting instability and droplet volume we performed a separate simulation in which we started with a tilted configuration and removed part of the liquid, thus reducing the droplet volume. In the subsequent equilibration, the tilted configuration gradually returned to the symmetrical geometry with the liquid droplet mounted on top of the nanowire as in Figure 1. This convincingly demonstrates that the symmetric wetting configuration is an equilibrium thermodynamic state for the smaller droplet volumes, and there is a critical volume at which a transition to a non-symmetric configuration occurs.

The observations above motivate the development of a wetting model to provide further insights into the nature of the tilting instability. We consider the 2d nanowire geometry illustrated in Figure 4a,b. Liquid-vapor and solid-liquid interfaces are assumed to be isotropic and therefore have circular shapes. The interfaces are connected at VLS triple junctions located on the side wall of the nanowire. We assume that the solid-liquid interface is mobile

and can adjust its shape to minimize energy, while the VLS triple junctions are restricted to move along the side walls. The wetting geometry is fully specified by a tilting angle α and two apparent wetting angles θ_s and θ_l defined in Figure 4b. The total surface free energy F^s of the system is given as

$$F^s = \gamma_{lv} L_{lv} + \gamma_{sl} L_{sl} + 2\gamma_{vs} L_{vs} \tag{1}$$

where γ_{lv}, γ_{sl} and γ_{vs} are liquid-vapor, solid-liquid and vapor-solid interface free energies, respectively and L_{lv}, L_{sl} and $2L_{vs}$ are the lengths of these interfaces.

We recognize that a two-dimensional fully isotropic treatment is a simplified model. However, the results that we obtain below will be sufficiently general to justify such an approximation. We will continue to use a three-dimensional vocabulary volume and area to represent their analogs in two dimensions: area and length.

To find the equilibrium wetting configurations we consider variations of shape subject to the constraints that the total volumes of the liquid and solid phases are constant

$$V_s = L_{vs} + \frac{R_{sl}^2}{2}\left(2\theta_s - \sin\left(2\theta_s\right)\right) \tag{2}$$

$$V_l = \frac{R_{lv}^2}{2}\left(2\theta_l - \sin\left(2\theta_l\right)\right) - \frac{R_{sl}^2}{2}\left(2\theta_s - \sin\left(2\theta_l\right)\right) \tag{3}$$

where R_{lv} and R_{sl} are the radii of curvature of the liquid-vapor and solid- liquid interfaces, respectively. By means of Eqs. (2) and (3), two variables from Eq. (1) can be eliminated, resulting in $F = F(\theta_s, \alpha, V_l, \left(\frac{\gamma_{lv}}{\gamma_{vs}}\right), \left(\frac{\gamma_{sl}}{\gamma_{vs}}\right))$. At a given set of isotropic surface tensions (i.e. the ratios $\left(\frac{\gamma_{lv}}{\gamma_{vs}}\right)$ and $\left(\frac{\gamma_{sl}}{\gamma_{vs}}\right)$) and fixed volume of the liquid V_l, the total surface free energy is a function of the apparent contact angle θ_s and the tilting angle α. The equilibrium configurations correspond to states with $\frac{\partial F}{\partial \alpha} = 0$ and $\frac{\partial F}{\partial \theta_s} = 0$. From these two equations, it can be derived that the following conditions are satisfied at equilibrium:

$$\gamma_{vs} = \gamma_{sl}\cos\left(\frac{\pi}{2} - \theta_s \pm \alpha\right) + \gamma_{lv}\cos\left(\theta_l \pm \alpha - \frac{\pi}{2}\right) \tag{4}$$

Eq. (4) can be interpreted as a balance of capillary forces at triple junctions in the direction parallel to the sidewalls of the nanowire, with plus and minus sign referring to each of the two triple junctions. The condition (4) is expected: because TJs parallel motion is not constrained, in equilibrium the net capillary force along this direction must be zero. The forces are not zero normal to the nanowire surface because the triple junction is pinned to the surface.

A typical free energy surface computed from Eq. 1 is illustrated in Figure 4c, with the three equilibrium states satisfying Eq. (4) illustrated as red, yellow and black points. The minimum (red point) corresponds to the stable wetting geometry of the nanowire. Note, that it is symmetrical, i.e., $\alpha = 0$, with contact angles that are determined by V_l, $\left(\frac{\gamma_{lv}}{\gamma_{vs}}\right)$ and $\left(\frac{\gamma_{sl}}{\gamma_{vs}}\right)$. These equilibrium angles are generally different from contact angles ϕ_{vs}^{Young} and ϕ_{lv}^{Young} for an unconstrained triple line given by Young's condition: $\gamma_{sl}/\sin\left(\phi_{sl}^{Young}\right) = \gamma_{vs}/\sin(\phi_{vs}^{Young}) = \gamma_{lv}/\sin(\phi_{lv}^{Young})$. In the nanowire geometry, for a given set of surface tensions, Young's condition appears at a critical liquid volume $V_l^{Young}\left(\left(\frac{\gamma_{lv}}{\gamma_{vs}}\right), \left(\frac{\gamma_{sl}}{\gamma_{vs}}\right)\right)$.

The black point in Figure 4c corresponds to the symmetrical ($\alpha = 0$) unstable wetting configurations, while the yellow sphere represents a saddle point configuration with $\alpha \neq 0$. This "tilted" state gives the lowest free

energy barrier for transition from the symmetric to asymmetric configurations, while the symmetrical transition path goes through the highest energy barrier and therefore it is the least likely path. The shape of the free energy surface depends on the droplet volume. As V_l increases the saddle point moves towards the minimum. At a critical volume V_l^{Young} the minimum and saddle points merge such that the Hessian of F becomes zero (c.f., Figure 4d) and the contact angles of the saddle configuration satisfy Young condition. At $V_l > V_l^{Young}$ no stable symmetric configuration exists and the system will undergo unstable evolution towards a tilted configuration. The value of the liquid volume giving rise to Young's angles can be calculated knowing $\left(\frac{\gamma_{lv}}{\gamma_{vs}}\right)$ and $\left(\frac{\gamma_{sl}}{\gamma_{vs}}\right)$. Thus, the function $V_l^{Young} = V_l^{Young}\left(\left(\frac{\gamma_{lv}}{\gamma_{vs}}\right), \left(\frac{\gamma_{sl}}{\gamma_{vs}}\right)\right)$ determines the stability limits: symmetrical wetting configurations of nanowires exist for droplet volumes $V_l < V_l^{Young}$, while they are unstable for $V_l > V_l^{Young}$. Changes in nanowire growth (i.e., environmental) conditions such as temperature, pressure or composition that modify surface free energies $\left(\frac{\gamma_{lv}}{\gamma_{vs}}\right)$ and $\left(\frac{\gamma_{sl}}{\gamma_{vs}}\right)$, in turn change V_l^{Young}. Thus, stable symmetrical nanowires, can become unstable and tilt upon such sudden changes in environmental conditions.

To interpret the role of the Young condition in determining the stability of symmetric nanowire wetting geometries we propose the following capillary force argument. For liquid droplet volumes $V_l < V_l^{Young}$ the net capillary forces *on* the vapor-solid-liquid triple junction (TJ) are normal to the sidewall of the nanowire, pointing inwards toward the solid putting the triple line in tension–the influence would be towards shortening the distance between the two triple points(c.f., Figure 5a). As a result any tilting perturbation is unfavorable as it leads to an increase in the distance between the TJs. At $V_l = V_l^{Young}$ the capillary forces are identically zero (c.f., Figure 5b). Finally, at $V_l > V_l^{Young}$ the capillary forces point surface away from the solid and the triple line is in compression: the triple junctions are pushed apart via tilting (c.f.,Figure 5c). This interpretation suggests an intrinsic link between the Young's force-balance condition and the stability of symmetric nanowire wetting geometries, which is expected to be more generally applicable, beyond the simple model considered above. Indeed, the correspondence between the predictions of the model and the MD observations for a system featuring pronounced interfacial anisotropies, suggest that the theoretical predictions are applicable to three dimensional systems with anisotropies characteristic of real VLS systems.

In summary, we have presented a theoretical analysis of equilibrium wetting geometries on single-crystal faceted solid nanowires, motivated by observations derived from three-dimensional MD simulations. The results suggest a tilting instability that is intrinsic to such geometries under conditions where the solid-liquid interface is deformable, while the solid/vapor nanowire surfaces remain flat. The transition from stable to unstable symmetric wetting geometries is shown to be governed by Young's condition and coincides with a change in the sign of the resultant force at the triple junction. This simple criterion links the stability of symmetric wetting geometries to the equilibrium contact angles that can be varied through changes in growth conditions such as temperature and partial pressure. It is suggested that the capillary instability described here is directly related to kinking processes observed experimentally in VLS nanowire growth, and that the Young's criteria discussed above provides a relatively simple guideline for choosing the experimental conditions required to realize straight versus kinked nanowire shapes.

Acknowledgments

This research was supported in part by the US National Science Foundation under Grant No. DMR-1105409. Use was made of computational resources provided under the Extreme Science and Engineering Discovery Environment (XSEDE), which is supported by the National Science Foundation under grant number OCI-1053575. T.F. was supported for part of this work by a post-doctoral fellowship from the Miller Institute for Basic Research in Science at University of California, Berkeley. W.C.C.'s effort was supported by a visiting Miller Faculty Fellowship, also from the Miller Institute for Basic Research in Science, during a sabbatical at the University of California, Berkeley.

Methods

Molecular dynamics simulations were performed using the LAMMPS software package. [19] To model nanowires wetted by liquid we used the angularly dependent Stillinger-Weber potential for Si. [20] First we prepared a simulation block with liquid and diamond-cubic solid phases separated by (111) solid-liquid interface. The interface plane was normal to the z direction of the simulation block, while the x and y directions were parallel to crystallographic directions $[1\bar{1}0]$ and $[11\bar{2}]$ of the solid phase, respectively. The dimensions of the simulation block were $30 \times 50 \times 30$ nm^3. The phases were equilibrated in a microcanonical (NVE) ensemble for 5 ns leading to a coexistence temperature of around 1682 K.

This simulation block was then used to produce input configurations for nanowire-liquid simulations. Specifically, we carved out columns with hexagonal crossection and $\{11\bar{2}\}$ side facets containing solid and liquid phases. The sizes of the solid surface facets ranged from 5 to 12 nm. To investigate the effects of the droplet size on equilibrium configuration, we varied the amount of liquid phase. The columns were then equilibrated during a 5 ns long simulation in a microcanonical . We performed up to 30 ns long simulations of equilibrated NW configurations. In equilibrium the amounts of solid and liquid phases do not change and the temperature fluctuates around equilibrium value.

Equilibrium simulations for an isolated droplet on a $\{111\}$ solid surface, shown in Figure 2b were performed in a microcanonical ensemble for 10 ns. [21] The solid slab used in these simulations had dimensions $2.3 \times 6.7 \times 32.9$ nm^3 parallel to $[1\bar{1}0]$, $[111]$ and $[11\bar{2}]$ crystallographic directions, respectively.

References

[1] R. S. Wagner and W. C. Ellis, Applied Physics Letters **4**, 89 (1964).

[2] Kenry, K.-T. Yong, and S. Yu, Journal of Materials Science , 1, 10.1007/s10853-012-6388-0.

[3] Y. Cui, Q. Wei, H. Park, and C. M. Lieber, Science **293**, 1289 (2001).

[4] K. W. Schwarz and J. Tersoff, Nano Letters **11**, 316 (2011).

[5] S. A. Dayeh, J. Wang, N. Li, J. Y. Huang, A. V. Gin, and S. T. Picraux, Nano Letters **11**, 4200 (2011).

[6] P. Madras, E. Dailey, and J. Drucker, Nano Letters **9**, 3826 (2009), PMID: 19860454.

[7] B. Tian, P. Xie, T. J. Kempa, D. C. Bell, and C. M. Lieber, Nat Nano **4**, 824 (2009).

[8] F. M. Ross, Reports on Progress in Physics **73**, 114501 (2010).

[9] E. J. Schwalbach, S. H. Davis, P. W. Voorhees, J. A. Warren, and D. Wheeler, Journal of Applied Physics **111**, 024302 (2012).

[10] E. Schwalbach, S. Davis, P. Voorhees, D. Wheeler, and J. Warren, Journal of Materials Research **26**, 2186 (2011).

[11] B. J. Carroll, Journal of Colloid and Interface Science **97**, 195 (1984).

[12] S. M. Roper, A. M. Anderson, S. H. Davis, and P. W. Voorhees, Journal of Applied Physics **107**, 114320 (2010).

[13] S. Muralidharan, P. W. Voorhees, and S. H. Davis, Journal of Applied Physics **114**, 114305 (2013).

[14] K. W. Schwarz and J. Tersoff, Phys. Rev. Lett. **102**, 206101 (2009).

[15] K. W. Schwarz, J. Tersoff, S. Kodambaka, Y.-C. Chou, and F. M. Ross, Phys. Rev. Lett. **107**, 265502 (2011).

[16] K. W. Schwarz and J. Tersoff, Nano Letters **11**, 316 (2011).

[17] R. Zucker, D. Chatain, U. Dahmen, S. Hagege, and W. Carter, Journal of Materials Science **47**, 8290 (2012).

[18] F. M. Ross, J. Tersoff, and M. C. Reuter, Phys. Rev. Lett. **95**, 146104 (2005).

[19] S. Plimpton, J. Comput. Phys. **117**, 1 (1995).

[20] F. H. Stillinger and T. A. Weber, Phys. Rev. B **31**, 5262 (1985).

[21] T. Frolov and Y. Mishin, Phys. Rev. Lett. **106**, 155702 (2011).

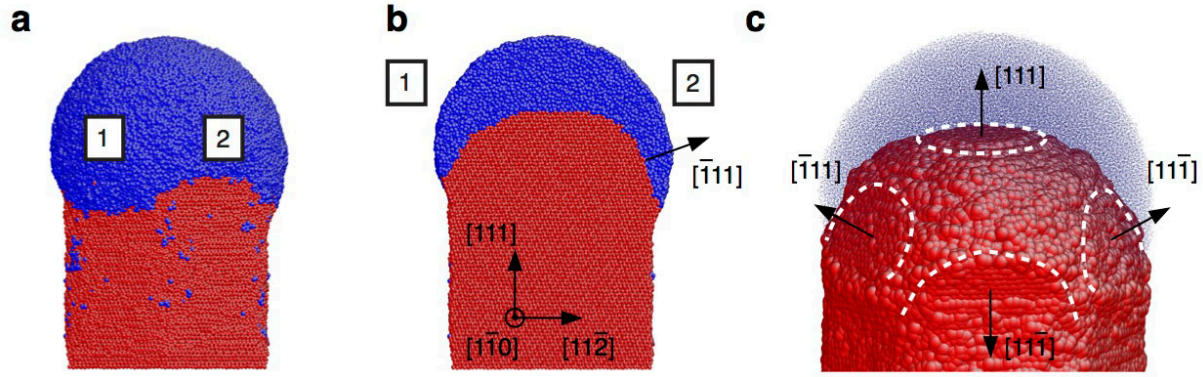

Figure 1: **Equilibrium wetting configurations of simulated nanowires. a,** Nanowire with solid (colored red) and liquid (blue) phases as identified according to a local crystalline order parameter. The solid-liquid-vapor contact line has a variable elevation as it traverses the perimeter of the nanowire: this triple line dips below the facets with $[\bar{1}11]$ and $[11\bar{1}]$ normals, and above the facet with $[1\bar{1}1]$ normal. Slice **b** shows the structure of the solid-liquid interface. **c,** A view of the solid liquid interface with semitransparent liquid phase illustrating its faceted nature.

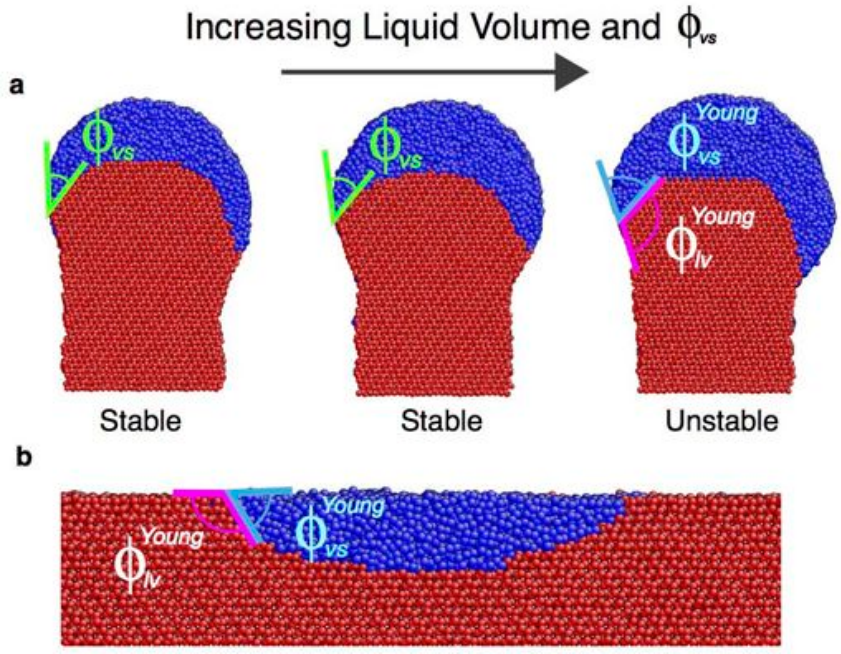

Figure 2: **Nanowires with increasing volume of the liquid droplet. a,** Equilibrium angles depend on the droplet volume, with ϕ_{vs} increasing with V_l. **b,** Equilibrium wetting angles of a liquid droplet on $[111]$ surface. Spontaneous tilting occurs when nanowire contact angles approach angles indicated in **b**.

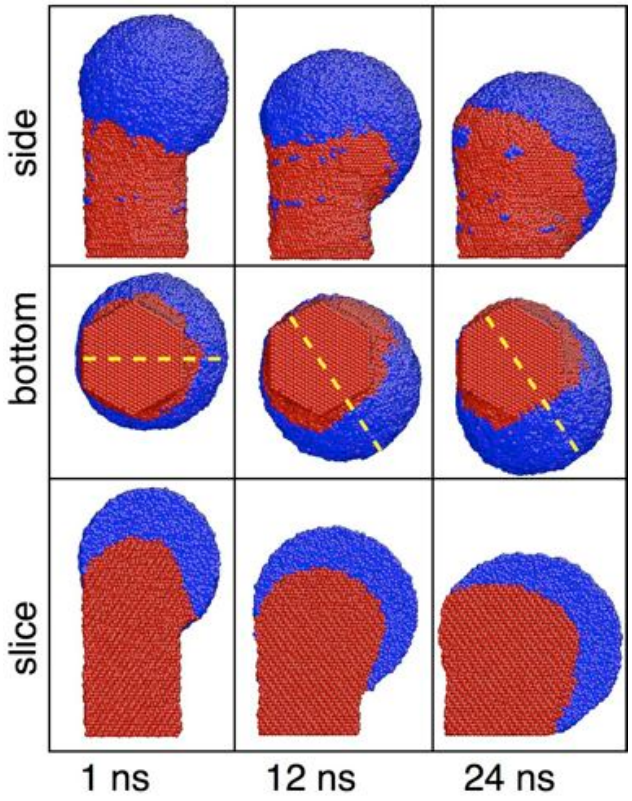

Figure 3: **Transition from symmetric to tilted configurations.** Time sequence of snapshots demonstrating the evolution of the droplet tilting during a 24 ns MD simulation. Top and middle panels show side and bottom views of the nanowire. The middle panel illustrates that the droplet tilting direction changes with time. The bottom panel shows slices going through the nanowire along planes marked in the middle panel by yellow dashed lines. Initially the tilting of the droplet leads to the formation of a large $[\bar{1}11]$ solid-liquid interface facet. At later times the droplet wets the side wall of the nanowire, with the solid-liquid interface becoming more rounded.

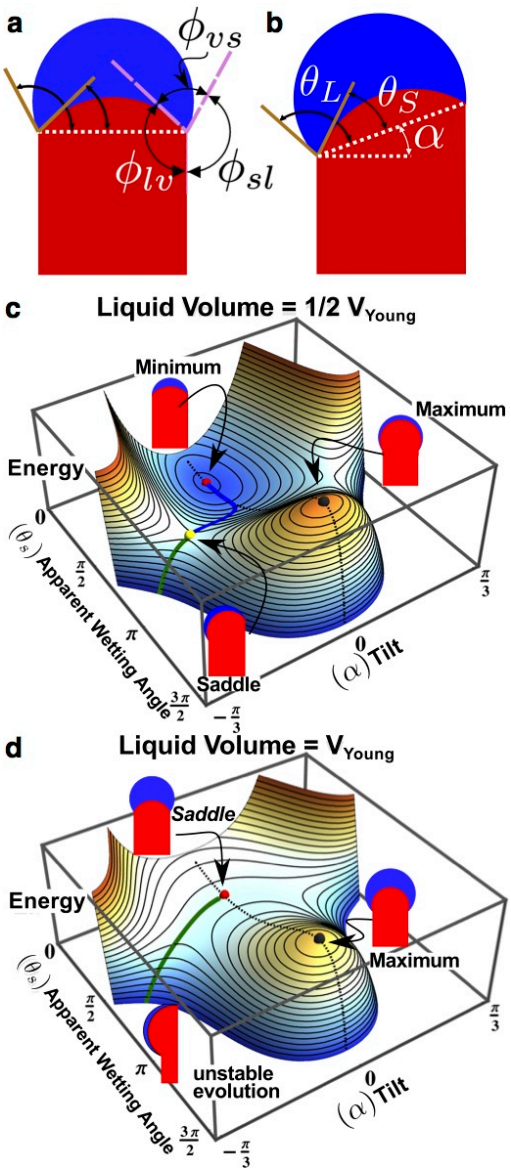

Figure 4: **Two Dimensional Model of Nanowire Capillary Instability. a,** The angles, ϕ , which vary with liquid volume. **b,** The model parameters that represent the degrees of freedom for capillary shapes: the asymmetric tilt angle α and the apparent wetting angle θ_s appear as coordinates in the free energy surfaces for different liquid volumes in the middle and bottom figure. For a symmetrical equilibrium configuration ($\alpha = 0$) $\phi_{vs} = \theta_L$ and $\phi_{lv} = \theta_s + \pi/2$. The free-energy surfaces are plotted for interface energy ratios $\gamma_{lv}/\gamma_{vs} = 9/10$ and $\gamma_{sl}/\gamma_{vs} = 3/10$. **c,** Free-energy surface plotted for a volume which is half of the Young's volume (i.e., the volume at which the ϕ_{ij} satisfy Young's equation). When $V_l < V_l^{Young}$, there is a metastable minimum at a finite θ_s and zero tilt angle ($\alpha = 0$), and symmetric saddle points for $\alpha \neq 0$. The blue and green lines were computed by steepest descent and represent the most probable path for the system to transform from a symmetric nanowire wetting geometry to a tilted configuration. **d,** As the volume increases, the saddle and metastable points approach each other and converge when $V_l = V_l^{Young}$. For liquid volumes larger than V_l^{Young} the metastable minimum corresponding to a symmetric nanowire geometry disappears, and symmetric configurations are unstable with respect to tilting.

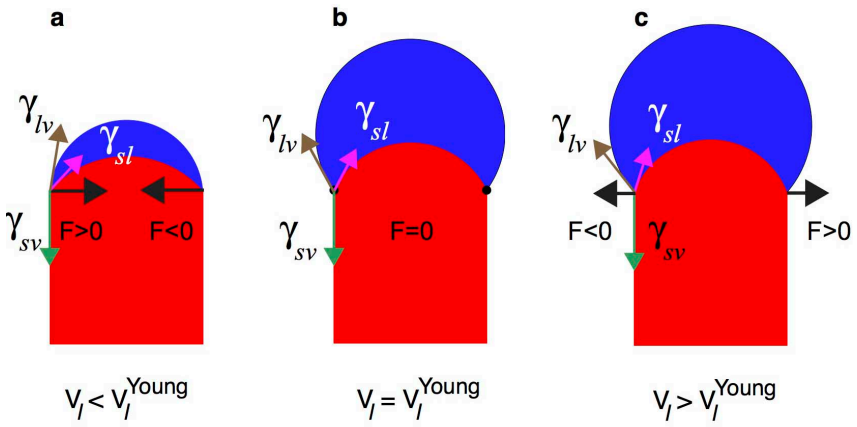

Figure 5: **Capillary forces on triple junctions.** The net capillary forces on triple junctions for different volumes of the droplet are shown by black arrows. These are result of the capillary forces from each of the three interfaces. **a,** Capillary force is directed normal to the nanowire axis and points inward towards the nanowire for $V_l < V_l^{Young}$. **b,** Zero force at Young's conditions. **c,** Capillary force is directed outward for $V_l > V_l^{Young}$. In case **a** capillary forces push triple junctions towards each other. Since tilting would increase the separation, it is not favorable. On the other hand, in case **c** a small perturbation from a symmetrical configuration will result in increasing tilting, since capillary forces try to pull the two triple junctions apart.